J. Biochem. 120, 1216-1223 (1996)

The Structure, Stability, and Folding Process of Amyloidogenic Mutant Human Lysozyme[1]

Jun Funahashi,* Kazufumi Takano,* Kyoko Ogasahara,* Yuriko Yamagata,† and Katsuhide Yutani*,[2]

**Institute for Protein Research, Osaka University, 3-2 Yamadaoka, Suita, Osaka 565; and †Faculty of Pharmaceutical Sciences, Osaka University, 1-6 Yamadaoka, Suita, Osaka 565*

Received for publication, August 12, 1996

The physicochemical properties of an amyloidogenic mutant human lysozyme (Ile56Thr) were examined in order to elucidate the mechanism of amyloid formation. The crystal structure of the mutant protein was the same as the wild-type structure, except that the hydroxyl group of the introduced Thr56 formed a hydrogen bond with a water molecule in the interior of the protein. The other physicochemical properties of the mutant protein in the native state were not different from those of the wild-type protein. However, the equilibrium and kinetic stabilities of the mutant protein were remarkably decreased due to the introduction of a polar residue (Thr) in the interior of the molecule. It can be concluded that the amyloid formation of the mutant human lysozyme is due to a tendency to favor (partly or/and completely) denatured structures.

Key words: amyloid formation, denatured state of a protein, human lysozyme, mutant protein, stability of amyloidogenic protein.

Amyloidosis is a heterogeneous group of disorders characterized by extracellular deposition of abnormal protein fibrils (*1*). Most amyloid fibrils consist of sulfated glycosaminoglycans and a variety of proteins in different forms of the disease. It has been proposed that conformational changes in amyloidogenic proteins lead to amyloid fibril formation and cause disease (*2*). Recently, mutant human lysozymes (Ile56Thr and Asp67His) have been reported to form amyloid deposits in the viscera, apparently causing hereditary non-neuropathic systemic amyloidosis, resulting in death by the fifth decade (*3*). The fact that lysozyme mutants form amyloid is exciting from the standpoint of understanding the mechanism of human amyloid formation, because there is a wealth of structural information and a good understanding of the folding pathway of the wild-type lysozyme (*2*). Because we have systematically studied a series of mutant human lysozymes in order to elucidate the mechanism of stabilization and folding of a protein in terms of its constituent amino acid residues (*4-9*), we took up this idea.

Human lysozyme is an $\alpha+\beta$ protein with 34% helical residues, and 11% β-strands. The amyloidogenic proteins that have been investigated regarding their physicochemical properties appear to have mainly β structure with a few α helices (*2*). As human lysozyme consists of a $\beta+\alpha$ N-terminal and all-helical C-terminal domains, the amyloidogenic mutant lysozyme may be a good example for understanding the relationship of amyloidogenesis to protein folding. In the wild-type human lysozyme structure, the side chain of Ile56 is completely buried in the interior hydrophobic core, while the amide group of the main chain hydrogen-bonds with one of the buried water molecules in the interior cavity near the hydrophobic core. To better understand amyloidogenesis, in this study we examined the crystal structure and physicochemical properties, such as stability and folding pathway, of an amyloidogenic mutant human lysozyme (I56T) . The replacement of Ile in the interior of a protein with Thr, including a polar group, did not affect the structure in the native state, but it did change the stability and the folding process. These findings have important implications for the mechanism of amyloidogenesis.

EXPERIMENTAL PROCEDURES

Materials—Mutagenesis, expression and purification of the mutant human lysozyme (Ile56→Thr) were performed as described (*4*). All other chemicals were of reagent grade.

The concentrations of the wild-type and mutant protein solutions were of determined spectrophotometrically using $E^{1\%}_{1cm}=25.65$ at 280 nm (*10*).

Assay of Lysozyme Activity—The lysis of *Micrococcus lysodeikticus* cells (0.2 mg/ml, Sigma) in 0.1 M potassium phosphate buffer (pH 6.2) was monitored at 450 nm and at 25°C (*11*).

Analytical Ultracentrifugation—The proteins were diluted in the same buffer including 0.1 M NaCl at various pHs. Sedimentation equilibrium was performed in a Beckman Optima XL-A analytical ultracentrifuge at 20,000 rpm at 10 or 37°C for 20 h. The partial specific volume was calculated to be 0.715 from the amino acid composition. The concentration gradients in the cells were determined

[1] This work was supported in part by Fellowships from the Japan Society for the Promotion of Science for Japanese Junior Scientists (K.T.) and by a Grant-in-Aid for Special Project Research from the Ministry of Education, Science, Sports and Culture of Japan (K.Y.).
[2] To whom correspondence should be addressed. Fax: +81-6-879-8616, Tel: +81-6-879-8615, e-mail: yutani@protein.osaka-u.ac.jp

spectrophotometrically at 280 nm.

Differential Scanning Calorimetry (DSC)—A DASM4 adiabatic microcalorimeter linked to an NEC personal computer was used for calorimetric measurements as described (*4*). The scan rate was 1.0 K/min. The sample solutions were prepared by dissolution in 0.05 M glycine buffer at pH 2.67, 2.98, and 3.11. The sample concentrations were 0.8 to 0.9 mg/ml.

X-Ray Crystallography—The mutant human lysozyme (I56T) was crystallized by gradually increasing the concentration of the reservoir solution (final concentrations 2.2 M NaCl, 20 mM acetate, pH 4.5) at 10°C using the hanging drop vapor diffusion method. The protein concentration in the droplet was 5.6 mg/ml. The crystals were isomorphous with the wild-type crystals. Diffraction data to 1.58 Å resolution were collected by the oscillation method on a Rigaku R-AXIS IIC mounted on a Rigaku RU-300 rotating anode generator (40 kV, 200 mA, Cu K_α) at 10°C. Data processing was performed with the programs provided by Rigaku. The data below 1.8 Å resolution were excluded from the refinements, due to their low accuracy and high R_{merge} value of *ca.* 18%. The starting model was based on the wild-type structure (*4*). The structure was refined using the program X-PLOR (*12*). The coordinates of the mutant human lysozyme have been deposited in the Brookhaven Protein Data Bank (ID code; 1OUA).

Equilibrium Studies—GuHCl-induced denaturation of the mutant protein was monitored by CD at 222 nm as described (*5*). CD measurements were carried out with a Jasco J-500 recording spectropolarimeter using a cell of 10 mm path length.

Kinetic Studies of Denaturation and Refolding—The reactions of denaturation and refolding were monitored by fluorescence intensity measurement above 300 nm with excitation at 280 nm. Fluorescence stopped-flow experiments were carried out with a Photal RA-401 stopped-flow spectrophotometer equipped with a mixing device using 1:10 volumes of 2 solutions (Ohtsuka Electronics). The systems for fluorescence measurement were as described previously (*5*).

All of the equilibrium and kinetic experiments were performed in 40 mM glycine-HCl buffer, pH 4.0, at 10°C.

RESULTS AND DISCUSSION

General Features of the Mutant Human Lysozyme (I56T)—The secretion efficiency in yeast of an amyloidogenic mutant human lysozyme (I56T) was about eight times lower than that of the wild-type protein. We obtained 12.5 mg of the purified mutant protein from a total of 61 liters of broth. The mutant human lysozyme was exhaustively dialyzed against distilled water and lyophilized for storage. This protein was soluble under all our experimental conditions, and a protein concentration of about 10 mg/ml could be used for crystallization. In contrast, the corresponding mutant (I55T) of hen egg lysozyme is remarkably less soluble than that of the wild-type protein (*14*). Human and hen egg lysozymes share 60% amino acid sequence identity, but the human lysozyme has a Gly residue inserted between positions 47 and 48 in the corresponding hen egg lysozyme. Therefore, the corresponding mutation of the hen egg lysozyme is I55T.

It has been reported that the wild-type hen egg lysozyme polymerizes reversibly with increasing pH at 20°C, and the dimer is the predominant form between pH 5 and 7 (*15*). To examine dimerization (polymerization) of the mutant and the wild-type human lysozyme, a sedimentation equilibrium run was performed by analytical ultracentrifugation at pHs 3.0, 6.5, 8.0, and 11.0. All the concentration gradients obtained for the mutant and the wild-type human lysozyme in the sedimentation equilibrium run at each pH could be well simulated on the assumption of the presence of a single species with a molecular weight of 14,700. This indicates that both proteins exist as monomers in solution under the conditions used. The distinction between the present results and those reported for hen egg lysozyme may be caused by differences in the protein concentration used or in the characteristics of the proteins. The protein concentration in the present study was 30–40 times lower than that in the case of hen egg lysozyme (*15*).

Circular dichroism (CD) spectra in the region from 250 to 200 nm of the mutant human lysozyme at pH 3, 6.5, 8.0, and 10.0 were identical with those of the wild-type human lysozyme (not shown). In the case of the hen egg mutant lysozyme (I55T), the ellipticity in the α-helical region around 220 nm of the CD spectrum is significantly reduced at pH 6.5 and 25°C, suggesting partial denaturation (*14*). These results suggest that the mutant human lysozyme (I56T) has different features from those of the mutant hen egg lysozyme (I55T).

Enzymatic activity of the mutant human lysozyme (I56T) was measured spectrophotometrically by turbidity assay at 450 nm, and was 78% of that of the wild-type protein.

The Crystal Structure of the Mutant Human Lysozyme (I56T)—Table I shows X-ray data collection and refinement statistics for the mutant human lysozyme (I56T). The mutant structure was essentially identical to the wild-type structure (*4*). The r.m.s. deviation for the main-chain atoms between the wild-type and mutant structures was 0.12 Å, which is comparable to the reported value of 0.09 Å between the wild-type and I56V structures (*4*). Figure 1 shows the superposition of the mutant structure on the wild-type structure in the vicinity of the mutation site. The

TABLE I. **X-ray data collection and refinement statistics for the mutant human lysozyme (I56T).**

A. Data collection	
Cell dimensions (Å)	
a	56.69
b	61.03
c	33.79
Resolution (Å)	1.8
No. of crystals	1
No. of measured reflections	28,187
No. of independent reflections	9,220
Completeness of data (%)	80.4
R_{merge} (%)[a]	5.6
B. Refinement	
No. of atoms	1,200
No. of solvent atoms	172
Resolution range (Å)	8–1.8
No. of reflections used	8,212
Completeness of data (%)	73.3
R factor[b]	0.148
r.m.s. of dev. (bond:Å)	0.009
r.m.s. of dev. (angle:°)	1.52

[a] $R_{merge} = 100 \times \Sigma|I - \langle I\rangle|/\Sigma\langle I\rangle$, [b] R factor $= \Sigma||Fo| - |Fc||/\Sigma|Fo|$.

striking feature is that the side chain of the threonine is rotated *ca.* 120° ($\chi 1$ angle, −47° in the mutant *vs.* −162° in the wild-type) so that the hydroxyl group of Thr 56 forms a hydrogen bond with one of the internal water molecules found in the wild-type and mutant structures. The hydrogen bonding distance is 3.06 Å. Other main-chain and side-chain movements in the vicinity of Thr 56 are somewhat larger than those in I56V, but the maximal shift except for the side chain atoms of Thr56 is only 0.32 Å for the oxgen atom of Gly55. Furthermore, the three internal water molecules near Thr56 move less than 0.25 Å.

Equilibrium Studies of Denaturation of the Mutant Human Lysozyme (I56T); Calorimetry and Denaturant Treatment—To examine changes in the conformational stability of the mutant human lysozyme (I56T) due to the substitution, we measured the heat stability and denaturation by guanidine hydrochloride (GuHCl). Figure 2 shows excess heat capacity curves resulting from differential scanning calorimetric recordings of the mutant human lysozyme (I56T) at acidic pH values (pH 2.67, 2.98, and 3.11) with that of the wild-type protein as a reference. The acidic pH region was chosen because of the high reversibility of the thermal denaturation of the mutant protein, as well as the wild-type protein. The denaturation temperature (T_d), the denaturation enthalpy changes [calorimetric (ΔH_{cal}) and van't Hoff (ΔH_{vH}) enthalpy changes], and the denaturation heat capacity change (ΔC_p) were obtained directly from analyses of the heat capacity curves (Table II). The denaturation temperature of the mutant protein decreased linearly with decreasing pH. The T_d value of the mutant protein was 12.5°C lower than that of the wild-type protein at pH 2.7 (Table III). The thermodynamic parameters of denaturation as a function of temperature can be calculated using Eqs. 1-3.

$$\Delta H(T) = \Delta H(T_d) - \Delta C_p(T_d - T) \quad (1)$$

$$\Delta S(T) = \Delta H(T_d)/T_d - \Delta C_p \ln(T_d/T) \quad (2)$$

$$\Delta G(T) = \Delta H(T) - T\Delta S(T) \quad (3)$$

where the ΔC_p value is assumed to be independent of temperature (*16*). Table III shows the denaturation thermodynamic parameters of the mutant and the wild-type proteins at the same temperature, 64.9°C, which is the denaturation temperature of the wild-type protein at pH 2.7. The result indicates that the decrease in Gibbs energy (ΔG) of the mutant protein is caused mainly by an enthalpic effect.

Makhatadze and Privalov have estimated the contributions of different interactions of each amino acid residue to enthalpy, Gibbs energy, and heat capacity increment on protein denaturation using model compounds (*17*). Calo-

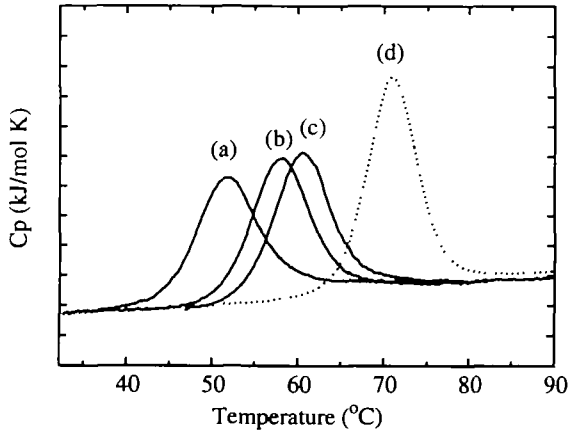

Fig. 2. **Excess heat capacity curves of the mutant human lysozyme (I56T) at pH 2.67 (a), 2.98 (b), and 3.11 (c). (d) represents that of the wild-type protein at pH 3.02 as a reference (*4*).** The increments in excess heat capacity were 10 kJ/mol K.

TABLE II. **Thermodynamic parameters for denaturation of the mutant human lysozyme (I56T) at different pH values.**

Protein	pH	T_d (°C)	ΔH_{cal} (kJ/mol)	ΔH_{vH} (kJ/mol)	Ratio $\Delta H_{cal}/\Delta H_{vH}$	ΔC_p[a] (kJ/mol·K)
I56T	3.11	60.52	408	432	0.94	4.8
	2.98	57.96	390	427	0.91	5.0
	2.67	51.78	367	380	0.97	4.2

[a] ΔC_p was obtained from each calorimetric curve.

TABLE III. **Thermodynamic parameters for denaturation of the mutant human lysozyme (I56T) at the denaturation temperature (64.9°C) of the wild-type human lysozyme at pH 2.7.**

Protein	T_d (°C)	ΔT_d (°C)	ΔC_p[a] (kJ/mol·K)	ΔH_{cal} (kJ/mol)	$\Delta\Delta G$ (kJ/mol)	Ratio $\Delta H_{cal}/\Delta H_{vH}$
Wild	64.9±0.5		6.6±0.5	477±4		0.95
I56T	52.4	−12.5	5.2±0.5	425±5	−15.2	0.94

[a] ΔC_p was obtained from the slope of ΔH against T_d.

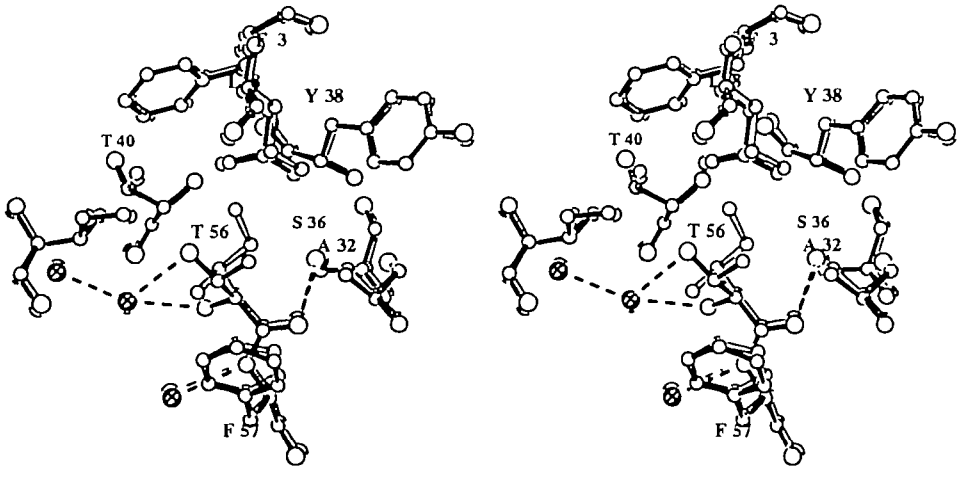

Fig. 1. **Stereo drawing showing (*13*) the mutant human lysozyme structure (I56T) in the vicinity of the mutation site.** The wild-type (open bonds) and mutant structures (filled bonds) are superimposed. Solvent water molecules are drawn as crossed-circles. Broken lines indicate hydrogen bonds.

rimetry and the X-ray structure of the mutant human lysozyme with valine at position 56 have already been reported (*4*). No change in the Val mutant structure (I56V) has been observed, except for the deletion of a methylene group. Table IV shows that the expected differences in ΔH and ΔG between the Val mutant and the wild-type human lysozymes using Makhatadze and Privalov's parameters are in good agreement with those obtained from calorimetric measurements. This agreement confirms that the conformational change of the mutant I56V is localized at the substitution site, as expected from the similarity of the structures obtained from X-ray analysis, and shows that Makhatadze and Privalov's parameters are reliable. The differences in hydration enthalpy and hydration Gibbs energy between Ile56 and Thr56 residues could be estimated to be −35.8 and −26.0 kJ/mol, respectively, at 65°C (Table IV), using Makhatadze and Privalov's parameters. This indicates that the observed large decrease in denaturation enthalpy change of the mutant I56T is mainly caused by the hydration enthalpy change of the polar group of Thr56 in the interior of the molecule. The decrease in Gibbs energy due to hydration of Thr56 was partly compensated by the hydrogen bonding energy of the hydroxyl group of Thr56 with water in the interior of the molecule, newly formed by the substitution. These results indicate that the mutant I56T is destabilized by the introduction of a polar residue in the interior of the protein and that the effect is mainly localized at the substitution site.

We also examined isothermal denaturation by a denaturant. Denaturation by GuHCl of the mutant human lysozyme was monitored by CD at 222 nm as a function of denaturant concentration at pH 4.0 and 10°C (Fig. 3). The transition curve of the mutant protein was highly cooperative at certain GuHCl concentrations, and the denaturation was completely reversible. The transition curve of the mutant protein was shifted to a lower concentration of GuHCl (about 1.3 M) than that reported for the wild-type protein (*5*), indicating that the mutant protein was remarkably destabilized by the substitution, in agreement with the result of heat denaturation. The transition curve was analyzed to evaluate the denaturation thermodynamic parameters using the following equation (*18*), assuming a two-state transition

$$\ln K_d = \ln K_d^{H_2O} + m_e[\mathrm{GuHCl}] \quad (4)$$

where K_d and $K_d^{H_2O}$ are the equilibrium constants for denaturation in any GuHCl concentration and in water, respectively, and m_e is a constant that is proportional to the increase in the degree of exposure of residues to the solvent upon denaturation. The denaturation Gibbs energy in water, $\Delta G_d^{H_2O}(=-RT\ln K_d^{H_2O})$, of the mutant protein was calculated to be 30.6 kJ/mol, which is 27.9 kJ/mol lower than that reported for the wild-type protein (*5*). Using calorimetric data and Eqs. 1-3, the denaturation Gibbs energies of the mutant (I56T) and the wild-type human lysozymes can be shown to be a function of temperature at pH 4.0 (Fig. 4). The extrapolated values (ΔG) to 10°C of the mutant (I56T) and wild-type proteins were 46.5 and 64.9 kJ/mol, respectively. Denaturation Gibbs energy values obtained from calorimetry and denaturant denaturation data did not coincide with each other at 10°C. The difference in extrapolated values using different methods (high temperature and high concentration of denaturant) might be

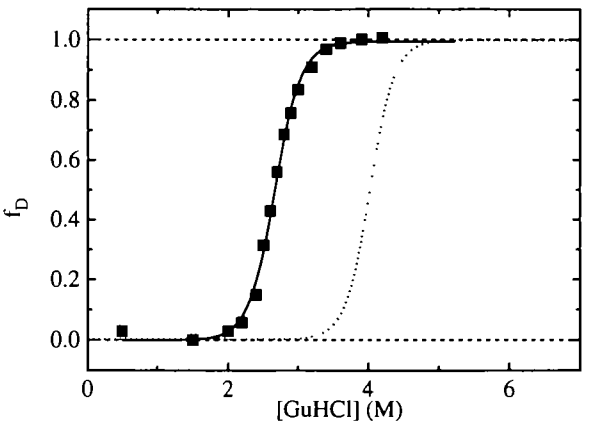

Fig. 3. **GuHCl denaturation curve of the mutant human lysozyme (I56T) (solid line) at pH 4.0 in 40 mM glycine HCl buffer and at 10°C and the wild-type protein (dotted line) (*5*) as a reference under the same conditions.** The fraction of denaturation (f_D) was calculated with the following equation: $f_D=([y]_n-[y])/([y]_n-[y]_d)$, where $[y]$ represents the CD value at 222 nm at a given concentration of GuHCl, and $[y]_n$ and $[y]_d$ are the CD values for the native and denatured states, respectively.

TABLE IV. **Contribution of different interactions of Ile, Val, and Thr residues at position 56 of human wild-type and mutant lysozymes to enthalpy and Gibbs energy on denaturation.** These values were calculated using parameters obtained by Makhatadze and Privalov (*17*).

	ΔH (kJ/mol)			ΔG (kJ/mol)		
	Ile56 (wild-type)	Val56	Thr56	Ile56 (wild-type)	Val56	Thr56
Hydration						
Polar surface			−35.8			−26.0
Aliphatic	−6.1	−5.1	−1.2	9.5	8.0	5.0
Interaction in the interior						
Hydrogen bond with water			(−13.3)			(23.1)
Aliphatic(van der Waals)	16.5	13.8	8.7	16.5	13.8	8.7
Total	10.4	8.7	(−41.6)	26.0	21.8	(10.8)
Expected values[a]		−1.7	(−52.0)		−4.2	(−15.2)
Measured values[b]		2.0	−52.0		−5.2	−15.2

[a]Expected values represent the difference between the total values of Val56 and the wild-type (Ile56). For example, −1.7=8.7 of ΔH (Val56) −10.4 (Ile56). [b]Measured values represent the difference between ΔH (or ΔG) measured by calorimetry of the Val56 (or Thr56) mutant and the wild-type (Ile56) proteins. The values in parentheses show the estimated values when the expected value of mutant I56T is assumed to coincide with the measured value. Based on this calculation we can estimate the contribution of the hydrogen bond of Thr56 with water in the interior of the protein.

caused by a difference in the denatured states. However, it can be concluded that the mutant human lysozyme (I56T) was much less stable than the wild-type protein over the entire temperature region shown in Fig. 4.

Kinetic Studies of Denaturation and Refolding of the Mutant Human Lysozyme (I56T)—To examine the effect of the substitution on the kinetic stability and the folding mechanism of human lysozyme, kinetic studies of the reversible denaturation-refolding of the mutant human lysozyme (I56T) were performed. The denaturation rate of the mutant protein was too fast to be monitored precisely in a stopped-flow apparatus at pH 3.0 and 25°C. Therefore, all measurements were performed at pH 4.0 and 10°C. The denaturation and refolding reactions were monitored by measuring aromatic fluorescence intensity. The denaturation of the mutant protein was followed on increasing the concentration of GuHCl from 0 M to various levels. The data were analyzed by use of the following equation

$$A(t) - A(\infty) = \Sigma A_i e^{-k_i t} \quad (5)$$

where $A(t)$ is the fluorescence intensity at a given time, and $A(\infty)$ is the value when no further change is observed; A_i is the amplitude of the ith phase, and k_i is the apparent rate constant of the ith phase. The denaturation kinetics of the mutant protein were described by a single exponential, as was reported for the wild-type protein (*5*). The kinetic amplitudes of the denaturation reactions at various final concentration of GuHCl were almost 100%. The logarithm of the apparent rate constant (k_{app}) of the mutant protein linearly increased with increasing GuHCl concentration as shown in Fig. 5. The k_{app} values of the mutant protein at all concentrations of GuHCl examined were 1-2 orders of magnitude higher than those of the wild-type protein, indicating that the substitution accelerates the denaturation rate of human lysozyme.

Refolding kinetics were studied by quickly diluting the 5 M GuHCl solution, in which the protein was completely denatured, to various GuHCl concentrations at 10°C and pH 4.0. The GuHCl concentration dependence of log k_{app} is also shown in Fig. 5, indicating that the refolding of the mutant protein has two phases below 1.5 M GuHCl, like that of the wild-type protein. The amplitude of the fast phase of the two phases observed in the refolding kinetics was greater than that of the slow phase, indicating that the fast phase is predominant in the refolding reaction. The k_{app} values of the major fast phase for the mutant protein were significantly lower than those of the wild-type protein, indicating that the substitution suppresses the refolding rate of human lysozyme.

Because the apparent rate constants for denaturation increased linearly with increasing GuHCl concentration, the relation between k_d (rate constant of denaturation) and GuHCl concentration can be inferred from Eq. 6, in which $k_d^{H_2O}$ is the rate constant in water (*19*).

$$\log k_d = \log k_d^{H_2O} + m_k [\text{GuHCl}] \quad (6)$$

k_d at a given GuHCl concentration can be obtained from the equilibrium constant of denaturation ($K_d = k_d/k_f$) and k_{app} ($= k_d + k_f$), where k_f is the rate constant of refolding. By fitting the data to Eq. 6, $k_d^{H_2O}$ and m_k were calculated to be 9.7×10^{-4} s^{-1} and 0.54 s^{-1}·M^{-1}, respectively, for the mutant human lysozyme. The value of $k_d^{H_2O}$ for the wild-type human lysozyme has been reported to be 1.5×10^{-6} s^{-1}. These results indicate that the rate of denaturation in water for the mutant protein was increased by 3 orders of

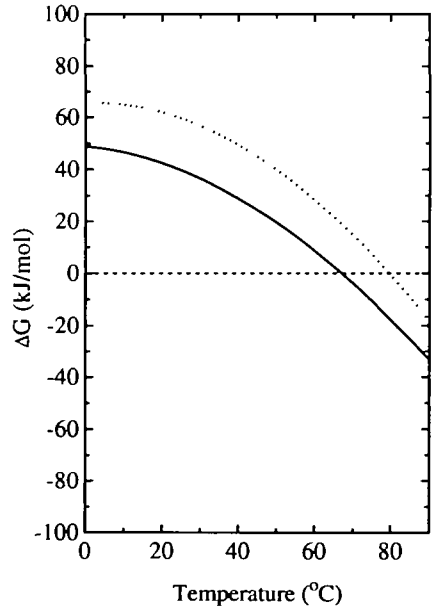

Fig. 4. **Temperature function of denaturation Gibbs energies of the mutant human lysozyme (I56T) (solid line) and the wild-type protein (dotted line) (*5*) at pH 4.0.** For the mutant protein, T_d at pH 4.0, ΔC_p, and ΔH at T_d were taken to be 67.0°C, 5.2 kJ/mol, and 435 kJ/mol, respectively. For the wild-type protein, T_d at pH 4.0, ΔC_p, and ΔH at T_d were taken to be 79.5°C, 6.6 kJ/mol, and 575 kJ/mol, respectively (*7*).

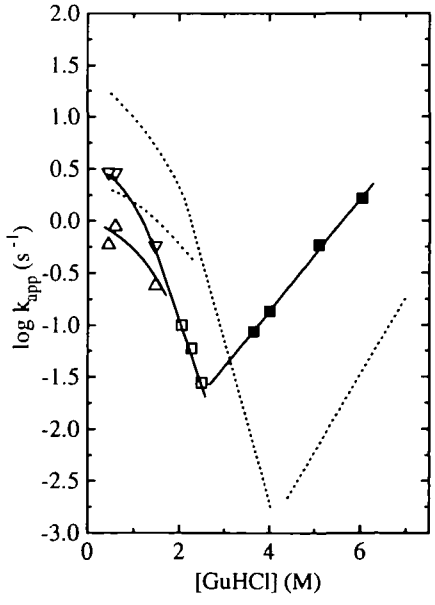

Fig. 5. **Dependence of the apparent rate constants (ln s^{-1}) of refolding (open symbols) and denaturation (filled symbols) for the mutant human lysozyme (I56T) on GuHCl concentration at pH 4.0 and 10°C.** Apparent rate constants of the mutant protein were measured in terms of fluorescence intensity above 300 nm with excitation at 280 nm. The open triangles (△) and (▽) refer to the slow and fast phases, respectively, in the biphasic refolding reactions. The broken lines show the refolding and denaturation phases of the wild-type protein (*5*) as a reference.

magnitude due to the substitution. If the protein folding reaction involves a reversible transition between two states, the denatured and native states, k_f of such a protein must follow the rate law (*19*)

$$\log k_f = \log k_f^{H_2O} - (m_e - m_k)[\text{GuHCl}] \quad (7)$$

where $\log k_f^{H_2O} = \log(k_d^{H_2O}/K_d^{H_2O})$. According to Eq. 7, $\log k_f$ can be calculated as a function of GuHCl concentration for a two-state transition using the denaturation kinetics and equilibrium data. Figure 6 shows that the experimental values of $\log k_{app}$ of the mutant protein upon refolding deviate from the curve predicted by the kinetics of a two-state equation. As reported for the wild-type and other mutant human lysozymes (*5, 6*), such a deviation indicates that a metastable intermediate is transiently produced during the refolding process and that the refolding phase reflects the transformation of the intermediate into the native form. The intermediate (I) is assumed to be similar to the molten globule state, which is less compact than a native protein, with a large amount of secondary and no tertiary structures (*20*). Hooke *et al.* have also confirmed the presence of a kinetic intermediate for human lysozyme using a pulse hydrogen exchange labeling method (*21*).

The folding pathway of the mutant human lysozyme may be written as follows.

$$D \Longleftrightarrow I \Longleftrightarrow N$$

The first stage corresponds to rapid formation of the molten globule (D→I), and the second stage is the organization of the specific tertiary structure (I→N). The first stage is known to be completed within a millisecond time range and could not be followed in this study, and the second stage involves the rate-determining step of the folding reaction. If we assume that the major fast refolding phase is the I→N reaction, we may obtain the activation Gibbs energies in water from the intermediate to the transition state using the extrapolated value to 0 M GuHCl of observed k_{app}. The activation Gibbs energy and kinetic data are correlated by the Eyring equation (*22*).

$$\Delta G^{\ddagger \cdot H_2O} = RT \ln (kT/h) - RT \ln k^{H_2O} \quad (8)$$

where k and h are the Boltzmann and Planck constants, respectively. The activation Gibbs energy in water for the denaturation, $\Delta G_d^{\ddagger \cdot H_2O}$, and for refolding, $\Delta G_f^{\ddagger \cdot H_2O}$, of the mutant protein are 15.2 kJ/mol lower and 3.3 kJ/mol higher, respectively, than those of the wild-type protein (Fig. 7). Gibbs energy profiles of the denaturation and refolding are shown in Fig. 7. Gibbs energy differences between the I and N states in the mutant (I56T) and the wild-type protein can be calculated to be 19.9 and 38.4 kJ/mol, respectively. Moreover, the difference in energy between the I and D states for the mutant protein (10.7 kJ/mol) was about half that of the wild-type protein (20.1 kJ/mol). Therefore, the energy profiles have the following implications. (i) The I state of the mutant protein is 18.5 kJ/mol more favorable than that of the wild-type protein, based on each N state. (ii) The I state of the mutant protein is more favorable due to the activation Gibbs energies for both denaturation and refolding reactions. (iii) The D state of the mutant protein is 9.4 kJ/mol more favorable than that of the wild-type protein, based on each I state. In conclusion, the mutant human protein is less stabilized than the wild-type protein at all steps in the folding process.

Why Is the Mutant Human Lysozyme (I56T) Amyloidogenic?—The native crystal structure and other biophysical properties examined in this study of the mutant human lysozyme (I56T) were similar to those of the wild-type protein. The mutant protein at acidic and alkaline pHs (pHs 3.0 and 11) was monomeric and was in the native form as judged from the CD spectra. In the native state, we could not find significant differences between the mutant and the wild-type human lysozymes. However, the mutant protein was greatly destabilized by the substitution. The denatured and intermediate states of the mutant protein were more

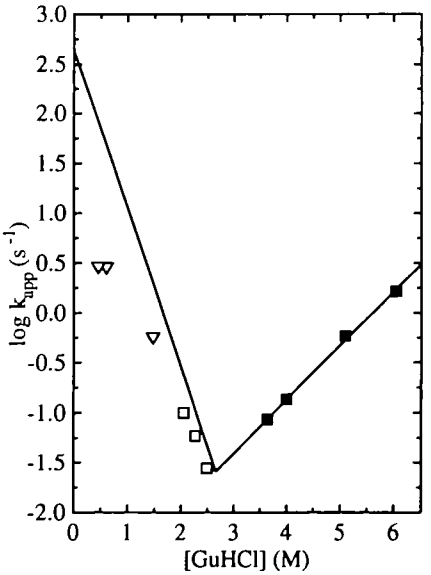

Fig. 6. **Dependence of the apparent rate constants of refolding and denaturation on GuHCl concentration in the mutant human lysozyme (I56T).** The solid line is that calculated for a simple two-state system [$K_d = k_d/k_f$ and $\log k_{app} = \log(k_d + k_f)$] (*19*). ▽ and □ are the experimental points for refolding kinetics (the fast phase in the two states). The symbols used here and the experimental conditions are the same as those in Fig. 5.

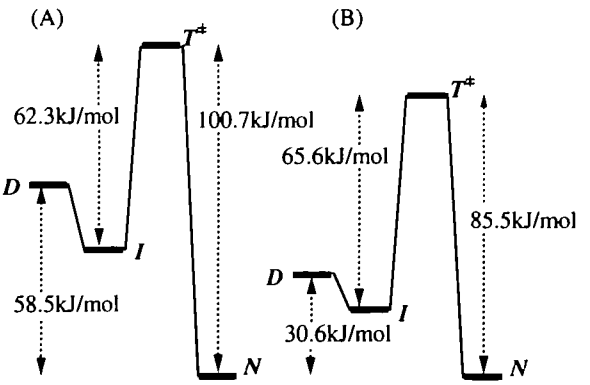

Fig. 7. **Gibbs energy profiles for the states in the folding pathway of the mutant human lysozyme (I56T) (B) and the wild-type protein (B) as a reference (*5*) in water.** $\Delta G_d^{H_2O}$ was calculated from the equilibrium denaturation studies. $\Delta G_f^{\ddagger \cdot H_2O}$ and $\Delta G_d^{\ddagger \cdot H_2O}$ were calculated from extrapolated values of k_f and k_d, respectively, to 0 M concentration of GuHCl, according to the Eyring equation. The species in the folding pathway are: N, the native state; T‡, transition state between the I and N states; I, the intermediate state; and D, the denaturant-induced denatured state.

favorable than those of the wild-type protein. These results show that conformations under partially or/and completely denaturing conditions might be suitable for amyloid formation.

The mutant human lysozyme at position 67 (Asp→His) has also been reported to be amyloidogeneic (*3*). The carboxyl group of Asp 67 forms hydrogen bonds with the hydroxyl group of Tyr54, the -OH group of Thr70, and a water molecule in the interior of the protein. This hydrogen-bond network is very important for the stabilization of this protein, because the deletion of one hydrogen bond due to the mutation Tyr54→Phe causes a large decrease in the stability (unpublished data). Therefore, we anticipated that the mutant D67H human lysozyme would be remarkably destabilized by the deletion of four hydrogen bonds. The locations of positions 67 and 56 in the native state are quite different from each other, suggesting that the common feature in forming amyloid deposits is not in the native conformation, but in the tendency to favor denatured structures. Dill and Shortle have suggested that the primary sequence of a protein is a major determinant of denatured conformation (*23*). The denatured conformation of the mutant human lysozyme might be responsible for amyloid formation.

It has been demonstrated that lysosomal extracts or lysosomal enzymes under acidic conditions could convert amyloidogenic proteins into amyloid (*24, 25*). On the other hand, in the case of transthyretin, the purified protein could be converted into amyloid fibrils *via* an acid-induced conformational change *in vitro* (*26, 27*). This demonstrates that conformational changes alone are sufficient to produce an intermediate capable of amyloidogenesis (*26, 27*). Although the mutant human lysozyme did not undergo conformational changes under acidic conditions, the destabilization of the protein should increase the proportion of denatured states under physiological conditions. Because denatured proteins and intermediates in the folding process are easily self-associated, unstable proteins might be candidates for amyloidosis (*2*).

We have studied the stability and denaturation/refolding process for many mutant human lysozymes (*4-9*). In the case of a disulfide-bond mutant (C77A/C95A), which exhibits 8-fold greater secretion in yeast compared with the wild-type protein, the stabilization of the molten globule state (the intermediate state) could correlate with the increase in secretion efficiency *in vivo* (*5*). On the other hand, the refolding rate of the mutant (C77A/C95A) is similar to that of the wild-type protein, though for the present mutant (I56T) the refolding rate was decreased, indicating that the destabilization mechanisms of both mutants (C77A/C95A and I56T) are different. If suitable conditions for artificial amyloid formation of human lysozyme are found, we could further establish the relationship between amyloidosis and protein folding.

A special feature of amyloid deposits is the universal presence of sulfated glycosaminoglycans which are probably laid down simultaneously with the fibrils (*1*). Although the significance of the sulfated glycosaminoglycans remains unclear, the interaction between sulfated glycosaminoglycans and the (partly) denatured state of amyloidogenic human lysozyme might be important for amyloid formation.

We thank Takeda Chemical Ind., Ltd. (Osaka) for providing plasmid pGEL125.

REFERENCES

1. Tan, S.Y. and Pepys, M.B. (1994) Amyloidosis. *Histopathology* **25**, 403-414
2. Kelly, J.W. (1996) Alternative conformations of amyloidogenic proteins govern their behavior. *Curr. Opin. Struct. Biol.* **6**, 11-17
3. Pepys, M.B., Hawkins, P.N., Booth, D.R., Vigushin, D.M., Tennent, G.A., Soutar, A.K., Totty, N., Nguyen, O., Blake, C.C. F., Terry, C.J., Feest, T.G., Zalin, A.M., and Hsuan, J.J. (1993) Human lysozyme gene mutations cause hereditary systemic amyloidosis. *Nature* **362**, 553-557
4. Takano, K., Ogasahara, K., Kaneda, H., Yamagata, Y., Fujii, S., Kanaya, E., Kikuchi, M., Oobatake, M., and Yutani, K. (1995) Contribution of hydrophobic residues to the stability of human lysozyme: Calorimetric studies and X-ray structural analysis of five isoleucine to valine mutants. *J. Mol. Biol.* **254**, 62-76
5. Taniyama, Y., Ogasahara, K., Yutani, K., and Kikuchi, M. (1992) Folding mechanism of mutant human lysozyme C77/95A with increased secretion efficiency in yeast. *J. Biol. Chem.* **267**, 4619-4624
6. Herning, T., Yutani, K., Taniyama, Y., and Kikuchi, M. (1991) Effects of proline mutations on the unfolding and refolding of human lysozyme: The slow refolding kinetic phase does not result from proline cis-trans isomerization. *Biochemistry* **30**, 9882-9891
7. Kuroki, R., Kawakita, S., Nakamura, H., and Yutani, K. (1992) Entropic stabilization of a mutant lysozyme (D86/92) induced by calcium binding. *Proc. Natl. Acad. Sci. USA* **89**, 6803-6807
8. Herning, T., Yutani, K., Inaka, K., Kuroki, R., Matsushima, M., and Kikuchi, M. (1992) Role of proline residues in human lysozyme stability: A scanning calorimetric study combined with X-ray structure analysis of proline mutants. *Biochemistry* **31**, 7077-7085
9. Kuroki, R., Inaka, K., Taniyama, Y., Kidokoro, S., Matsushima, M., Kikuchi, M., and Yutani, K. (1992) Enthalpic destabilization of a mutant human lysozyme lacking a disulfide bridge between Cys-77 and Cys-95. *Biochemistry* **31**, 8323-8328
10. Parry, R.M., Chandan, R.C., and Shahani, K.M. (1969) Isolation and characterization of human milk lysozyme. *Arch. Biochem. Biophys.* **130**, 59-65
11. Yoshimura, K., Toibana, A., Kikuchi, K., Kobayashi, M., Hayakawa, T., Nakahama, K., Kikuchi, M., and Ikehara, M. (1987) Differences between *Saccharomyces cerevisiae* and *Bacillus subtilis* in secretion of human lysozyme. *Biochem. Biophys. Res. Commun.* **145**, 712-718
12. Brunger, A.T. (1992) X-PLOR Manual Ver. 3.1. Yale University, NH, USA
13. Johnson, C.K. (1976) ORTEPII: A Fortran thermal-ellipsoid plot program for crystal structure illustration. Oak Ridge National Laboratory, TN, USA
14. Shih, P., Holland, D.R., and Kirsch, J.F. (1995) Thermal stability determinants of chicken egg-white lysozyme core mutants: Hydrophobicity, packing volume, and conserved buried water molecules. *Protein Sci.* **4**, 2050-2062
15. Sophianopoulos, A.J. and Van Hole, K.E. (1964) Physical studies of muramidase (lysozyme). II. pH-Dependent dimerization. *J. Biol. Chem.* **239**, 2516-2524
16. Privalov, P.L. and Khechinashvili, N.N. (1974) A thermodynamic approach to the problem of stabilization of globular protein structure: A calorimetric study. *J. Mol. Biol.* **86**, 665-684
17. Makhatadze, G. and Privalov, P. (1995) Energetics of protein structure. *Adv. Protein Chem.* **47**, 307-425
18. Pace, C.N., Grimsley, G.R., Thomson, J.A., and Barnett, B. (1988) Conformational stability and activity of ribonuclease T1 with zero, one, two intact disulfide bonds. *J. Biol. Chem.* **263**, 11820-11825
19. Matouschek, A., Kellis, J.T., Jr., Serrano, L., Bycroft, M., and Fersht, A.R. (1990) Transient folding intermediates characterized by protein engineering. *Nature* **346**, 440-445

20. Kuwajima, K. (1989) The molten globule state as a clue for understanding the folding and cooperativity of globular-protein structure. *Proteins Struct. Funct. Genet.* **6**, 87-103
21. Hooke, S.D., Radford, S.E., and Dobson, C.M. (1994) The refolding of human lysozyme: A comparison with the structurally homologous hen lysozyme. *Biochemistry* **33**, 5867-5876
22. Frost, A.A. and Pearson, R.G. (1961) Transition-state theory: Comparison of collision and transition state theories in *Kinetics and Mechanism*, 2nd ed., pp. 93-99, John Wiley and Sons, New York
23. Dill, K.A. and Shortle, D. (1991) Denatured states of protein. *Annu. Rev. Biochem.* **60**, 795-825
24. Glenner, G.G., Ein, D., Eanes, E.D., Bladen, H.A., Terry, W., and Page, D.L. (1971) Creation of amyloid fibrils from Bence Jones proteins *in vitro*. *Science* **174**, 712-714
25. Shirihama, T., Miura, K., Ju, S.T., Kisilevsky, R., Gruys, E., and Cohen, A.S. (1990) Amyloid enhancing factor-loaded macrophages in amyloid fibril formation. *Lab. Invest.* **62**, 61-68
26. Colon, W. and Kelly, J.W. (1992) Partial denaturation of transthyretin is sufficient for amyloid formation *in vitro*. *Biochemistry* **31**, 8654-8660
27. Colon, W. and Kelly, J.W. (1991) Transthyretin acid induced denaturation is sufficient for amyloid formation *in vitro* in *Applications of Enzyme Biotechnology*. (Kelly, J.W. and Baldwin, T.O., eds.) pp. 99-108, Plenum, New York